

Spinodal decay of a liquid mixture under conditions of inhibited convection—restorability of the spatial structure

A. V. Antonov, N. F. Bunkin, A. V. Krasnoslobodtsev, A. V. Lobeev, G. A. Lyakhov, and A. I. Malyarovskii

General Physics Institute, Russian Academy of Sciences, 117942 Moscow V-333, Russia

(Submitted 4 February 1993)

Zh. Eksp. Teor. Fiz. **104**, 2761–2773 (August 1993)

Using a thin-layered geometry we observed in an experiment about the transition of a stratified mixture with a lower critical point (2,4,6-trimethylpyridine + water) to the labile region the effect of a temporally quasiperiodic change in the scales of the structure occurring during the spinodal decay. A theoretical model connects these dynamics with a flow mechanism for the spatial phase separation in liquid solutions.

INTRODUCTION

A physical mixture can be in three qualitatively different states (see the survey in Ref. 1); the regions in which they are realized in the phase diagram (Fig. 1) are delimited by the binodal b (in its points the chemical potentials of two equilibrium phases are equal) and the spinodal s (on it the interdiffusion coefficient of the components of the mixture vanishes). In the region I which lies outside the binodal the state with a uniform spatial distribution of the density u is stable; in the metastable region II diffusion guarantees the motion to one of the uniform states which is selected by spontaneous symmetry breaking. In the labile region III the diffusion coefficient is negative so that any spatial fluctuation is amplified and the ground state turns out to be spatially inhomogeneous and characterized by a well defined ordering. The realization of such a state when one passes through the spinodal is called spinodal decay.

The observed state of a mixture depends in a well defined way on the external conditions, in particular on the dynamics of these conditions. For instance, to observe the spinodal decay when there is a transition from the state 1 of an actual mixture to the point 2 (see Fig. 1) the corresponding change in temperature (or pressure) must be sufficiently fast for diffusion not to be able to extend the nuclei of conjugate phases (the states 3 and 4 and all intermediate states such as 3' and 4') to a size which is critical for stratification due to convection. The requirements for the speed of the transition to the labile state are very rigid: it suffices to note that solely the determination of the position of the spinodal in the phase diagram forces us to apply either extrapolation methods² acting only in the direct vicinity of the critical point T_c where the binodal and the spinodal touch each other, or nontrivial means for a fast change of the thermodynamic parameters (e.g., light-induced³ or due to strong mixing⁴). These requirements become more stringent when the "immersion depth" into the labile region becomes greater—in a cell of about 1 cm size a mixture stratifies after 15 minutes for $\Delta T(I \rightarrow 2) \sim 10^{-3}$ K, but after a few seconds for $\Delta T(I \rightarrow 2) \sim 1$ K. The speed with which the ordered decay structure spreads out due to convective counterflow of the light and the heavy phases decreases when the viscosity of

the mixture increases or when the difference in density of the conjugate phases decreases; these, however, are essentially uncontrolled parameters barring exceptional cases. An experiment carried out in a state of weightlessness would be ideal.

An alternative that is used in our experiment consists in the choice of a thin-layer vertical geometry for the cell with the mixture to be studied (the distance between the windows is $d = 50 \mu\text{m}$). The surface tension forces considerably inhibit the convection here. The lifetime of the spinodal decay structures is then increased to tens of minutes for $\Delta T(I \rightarrow 2) \sim 1$ to 10 K. It is necessary here to give an explanation. Of course, the suppression of the convection does not strictly affect the process of the formation of new phases. However, if there is no convection these phases are not separated in real space and conjugate phases in the form of nuclei or droplets coexist in a thin cell in the mixed state. If we choose some sufficiently small region in the cell the density of the components of the mixture of the two phases, averaged over that region, will be equal to the initial density of the mixture (i.e., before the transition to the labile region). This is the principal reason for the special place of thin cells for a study of spinodal decay in preference to extended ones: in thin cells one can realize a labile state on average in a small region which exists for a rather long time.

In the first observation of the spinodal decay⁵ in a liquid (centimeter cell, methanol + cyclohexane mixture) they, firstly, recorded, the occurrence of the ordered structure itself in the mixture which made the transition into the labile region by means of a thermostat: during the scattering of a beam from a He-Ne laser passing through the mixture there appeared in the far zone apart from the central spot a ring caused by the scattering by the short-range order structure; the radius of this ring is inversely proportional to the size of the inhomogeneity arising as the result of the decay. Secondly, it was shown that the ring in the scattering field contracted with time, i.e., in agreement with the linearized theory of density fluctuations (see Ref. 6) the scale of the structure increased. The conditions of the experiment of Ref. 5 and similar ones, however, limited the possibilities for studying the kinetics of the spinodal decay because the duration of these experiments cannot

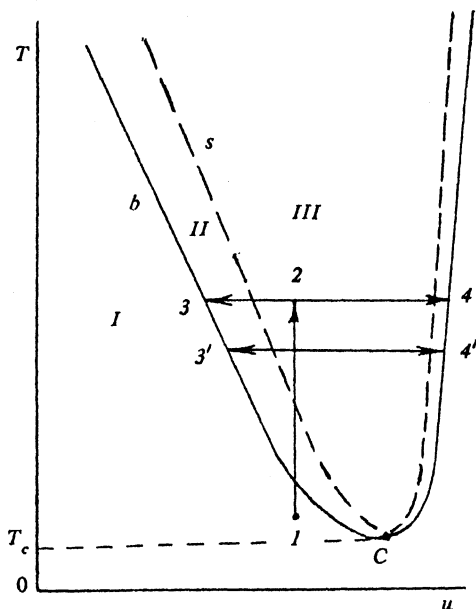


FIG. 1. Phase diagram of the aqueous mixture of 2,4,6-trimethylpyridine.

exceed the convective layering time. The conclusion that the dynamics of the decay was monotonic in time holds therefore only within the limits of a rather short time interval. On the other hand, the theory of Ref. 6 is restricted by the assumption that the deviations of the local density from the equilibrium one are small; its prediction of the monotonicity of the decay process which is diffusive in its nature is essentially already predetermined by this assumption. The kinetics under conditions of a strong nonlinearity, taking into account the density dependence of the relaxation times, may be nontrivial as in other self-organizing systems (see, e.g., Ref. 7).

We have already noted that the experiment described below was carried out under conditions when the convective mixing which naturally disrupts the decay process was greatly inhibited. To interpret the studies in this mixture of the kinetics of the spinodal decay which is, generally speaking, nonmonotonic we have developed a nonlinear theory, generalizing Ref. 6 and describing qualitatively the various kinetic regimes: relaxation to an equilibrium level, soliton transmission, and cnoidal waves.

1. EXPERIMENT TO OBSERVE THE SPINODAL DECAY IN AN ASSOCIATED WATER MIXTURE

The experiment was carried out with a water mixture of 2,4,6-trimethylpyridine (TMP) (Fig. 1). This compound belongs to a biologically important class of azines, to which the nucleotides DNA and RNA, and a number of vitamins and medicines belong. The physical properties of the TMP mixtures are to a large extent determined by the kinetics of the hydrogen bonds between the nitrogen atoms in the pyridine rings in the TMP molecules and the hydrogen atoms in the water molecules. In particular, these bonds guarantee the stratification at low temperatures (the

mixture has a lower critical point equal to $T_c = 5.7^\circ\text{C}$). The mixture with an initial density corresponding to the critical one (97 molecular % of H_2O) was placed in a cell.

The cell consisted of two circular quartz windows with a distance between them given by the thickness of the packing and equal to $50\ \mu\text{m}$. The kinetics of the mixing in it was determined practically solely by diffusion, i.e., for a deep approach into the labile region in our experiments we did not need special fast means to change the temperature; the temperature was changed by means of a normal thermostat. The quartz windows with drops of the liquid to be studied between them were clamped in a circular metallic ring fitted with a water jacket. The depth of the ring was equal to the two quartz windows joined in height while its diameter was larger by $0.5\ \text{mm}$ than the diameter of the quartz windows, i.e., there was a free volume between the quartz windows and the ring itself. In the compression process the liquid filled the space between the windows uniformly and was squeezed into the volume between the ring and the quartz windows, filling it and thereby guaranteeing thermal contact between the ring (water jacket) and the faces of the windows. The temperature front propagated during heating from the faces of the windows along their radius (see Fig. 2).

The time for establishing thermal equilibrium in the mixture, determined experimentally from the speed at which the external surface of the windows of the cell is heated up was about 10 minutes. The heating up of the liquid itself proceeds faster because there is no contact with the air. The initial stage of the decay is then partially superimposed on the final heating process so that a quantitative comparison of the experimental result with theory can here not be exact. This is the price to be paid for the possibility that the mixture can make a transition to the region of states far from the spinodal; we note that no qualitative differences were observed between theory and experiment for the dynamics of the decay in the stationary regime.

Up to the start of the experiment the temperature of the mixture in the cell was sustained at a level below T_c by means of a thermostat connected with the water jacket of the cell. After the recording instrument was tuned up (see below) for a few seconds the water in the thermostat was warmed up to 25 to 30°C , which corresponds to deep penetration into the labile region. The moment the thermostat was switched on to heating served as the moment from which the time is reckoned in the experiment.

The experimental set-up is sketched in Fig. 2. Radiation (1) from a single-mode He-Ne laser with a Gaussian profile (formed by means of a so-called "soft" diaphragm) and a plane-parallel beam (the diameter of the spot formed by a telescope was about $1.5\ \text{cm}$) passed through the cell (2) with the mixture to be studied. Immediately behind the cell a collecting lens (3) was placed with a focal distance of $4\ \text{m}$ and an aperture diameter of $22.5\ \text{cm}$. This lens, firstly, collected the rays scattered not only by large-scale structures (i.e., at small angles), but thanks to the large aperture also by rather small-scale structures. Secondly, it guaranteed the far zone for observing the pattern

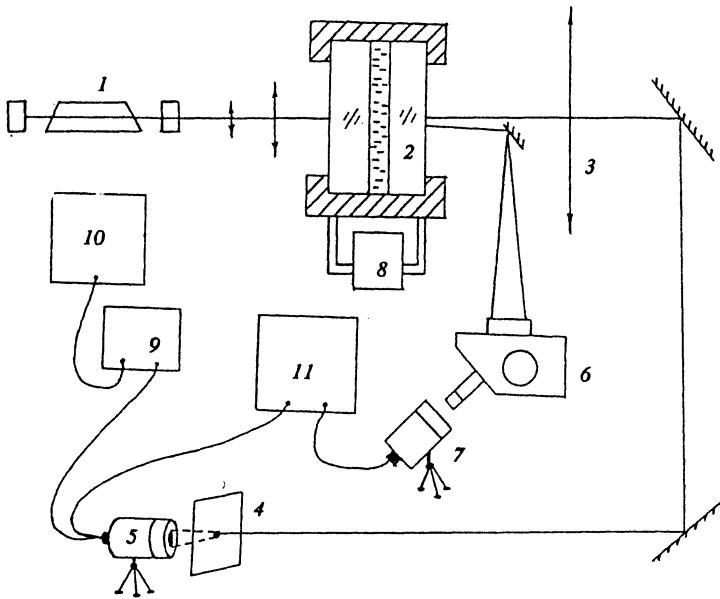


FIG. 2. Sketch of the experimental set-up. (1): He-Ne laser; (2): cell with mixture to be studied; (3): wide-aperture long-focus lens; (4): mask; (5) and (7): television cameras; (6): microscope; (8): thermostat; (9): analog-to-digital converter; (10): computer; (11): television monitor.

of the scattered radiation. In the focus of this lens a circular mask (4) was placed completely overlapping the zeroth maximum of the scattered beam, and behind the mask a television camera (5) was placed with an aperture diameter of 2 cm. The mask eliminated the incidence onto the television camera of the strong, but uninformative light signal from the direct beam. At the same time a separate section of the cell was projected onto another television camera (7) by means of a microscope (6). This made it possible to observe in parallel the dynamics of the structures appearing in the cell and the angular spectrum of the scattering of the laser beam by those structures. Photographs (Fig. 3) obtained by means of the microscope illustrate the development of the structures arising during the spinodal decay. Initially (for a time $t \sim 1$ min after the thermostat (8) has been switched on) the front of the spinodal decay wave appears moving across the cell, and behind the front one can see small cellular structures with a size of 1 to 10 μm (Fig. 3a); after that the structures become larger in the whole field of observation to reach a size of up to 100 μm ($t = 2.5$ min, Fig. 3b) and, finally, these 100 μm cells combine into an aggregate of about 1 cm ($t = 5$ min, Fig. 3c).

The signals from the television camera (5) which correspond to the scattering spectrum were processed by a computer (10) after passing through an analog-to-digital converter (9). In the processing the analog signal corresponding to the normal television frame was digitized with a time interval of 1 or 5 s during the whole of the experiment (about 20 min from the moment the thermostat is switched on to heating). We show in a photograph (Fig. 4) an example of the digitized representation of the scattering spectrum. The sharp circle on the left in which there clearly are no reflections corresponds to the mask (4) which overlaps with the zeroth maximum of the radiation; the light which can be seen to the right of the mask corresponds to scattering by structures appearing during the spinodal decay. We note that the pattern of the scattering

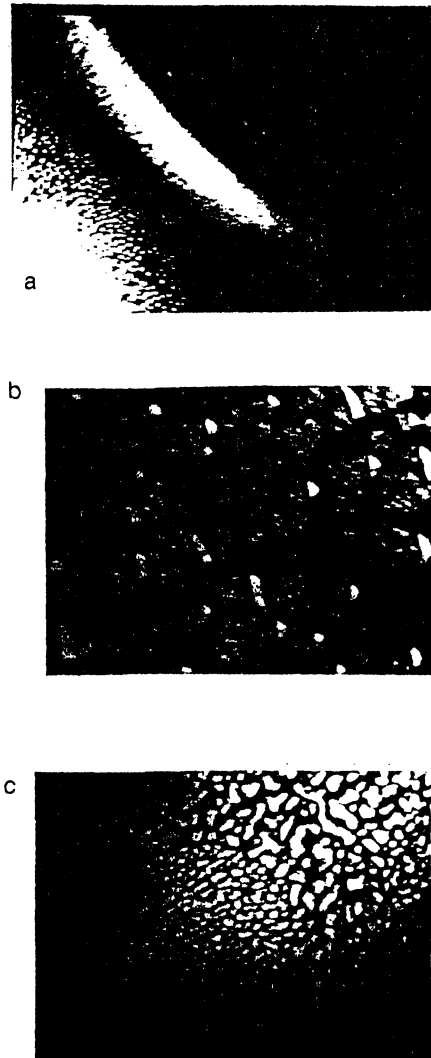


FIG. 3. Microphotographs of the spinodal decay at different times after the start of the heating: $t = 1$ min (a); 2.5 min (b); 5 min (c).

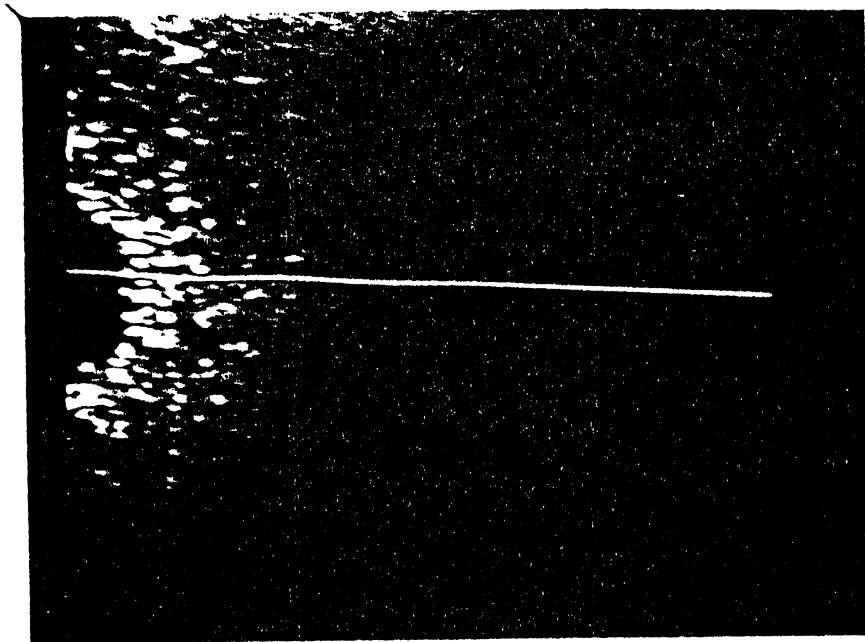


FIG. 4. Photograph of the digitized image of the scattering spectrum.

changes at each moment of time. A larger size corresponds to a reflection positioned in this photograph closer to the image of the mask. The size of a scattering structure can, if necessary, be determined exactly. To do this one must replace the cell with the mixture by, for instance, a diffraction lattice with a known spacing and digitize its angular scattering spectrum, thus comparing a known size of scatterer and the location of the reflection from this scatterer on the entrance pupil of the television camera. Taking the mask into account the processing system recorded reflections corresponding to structures from 20 to 300 μm . The computer read out the brightness of the frame along a chosen television line (see photograph); the television line along which the image was processed was strictly fixed during the whole duration of the experiment.

A typical series of angular spectrum densitograms obtained in this way gives the following picture of the development of the spinodal decay with time (Fig. 5). Up to the time $t \sim 1$ min from the start of the heating the density distribution remains uniform and there are no reflections. Initially the decay corresponds to the appearance of reflections in the whole of the field of the television camera (Fig. 5a, $t = 1.5$ min). When time goes on the small structures disappear and one can only see reflections corresponding to sizes of from 300 to 60 μm (Fig. 5b, $t = 2.8$ min). Further, the scattered light disappears practically from the field of the television camera since the structures become so large that the mask already overlaps the reflection from them (Fig. 5c, $t = 2.9$ min). Densitograms corresponding to later times clearly demonstrate that the process is periodic a pattern characteristic of average- and large-size structures with sizes of 50 to 300 μm ($t = 3.5$ and 12.8 min) again appears; later on ($t = 6.2$ and 16.1 min) we have the already familiar pattern with three clearly expressed reflections (compare Figs. 5b, 5e, and 5g).

The processing of densitograms of the angular spectra like Fig. 5 from a series of observations of a 20 min dura-

tion (as we stated already the densitograms were plotted with intervals of 5 or 1 s, i.e., the body of data for processing included 240 or 1200 densitograms) gives us the dynamics of the light scattering by structures of given sizes. We measured in each densitogram the intensity of the radiation scattered by 60 μm and 30 μm structures and we have constructed in Fig. 6 the time-dependence of these intensities; to eliminate temporal fluctuations in the brightness of the television signal each ordinate is here averaged over several successive densitograms. This function also has a periodic character. For the reflection of 60 μm structures (Fig. 6a) growth and decline of the intensity alternate with one another, both in the not yet established thermal regime (the times $t \sim 2$ and 6 min correspond to the appearance of the triple of characteristic reflections of Fig. 5) and in a regime which is steady as far as temperature is concerned: for $T \geq 10$ min growth, decline, and exit to a quasiconstant intensity level also occur (the time to return to a three-reflection regime is $t \sim 16$ min). The dynamics of the intensity of the scattering from 30 μm structures has a qualitatively similar character (Fig. 6b). At the same time there are quantitative differences between them: during the measuring time only two "spikes" rather than three, as for the 60 μm structures, are observed here in the scattering intensity. The quasiperiod of the spinodal decay therefore depends on the size of the decaying structure. A decisive role may here be played also by the fact that the layer thickness of the mixture in the cell is 50 μm . An important conclusion consists, firstly, in that the dynamics of the spectra is practically independent of the process by which the thermal regime is established. Secondly, the spinodal decay clearly demonstrates the "restorability" which is well known in the physics of nonlinear systems (see, e.g., Ref. 7). This is just a nonlinear effect, i.e., decisive in the decay are diffusive rather than wave processes. Its description requires a generalization of the theory of Ref. 6, taking into account the density dependence of the parameters.

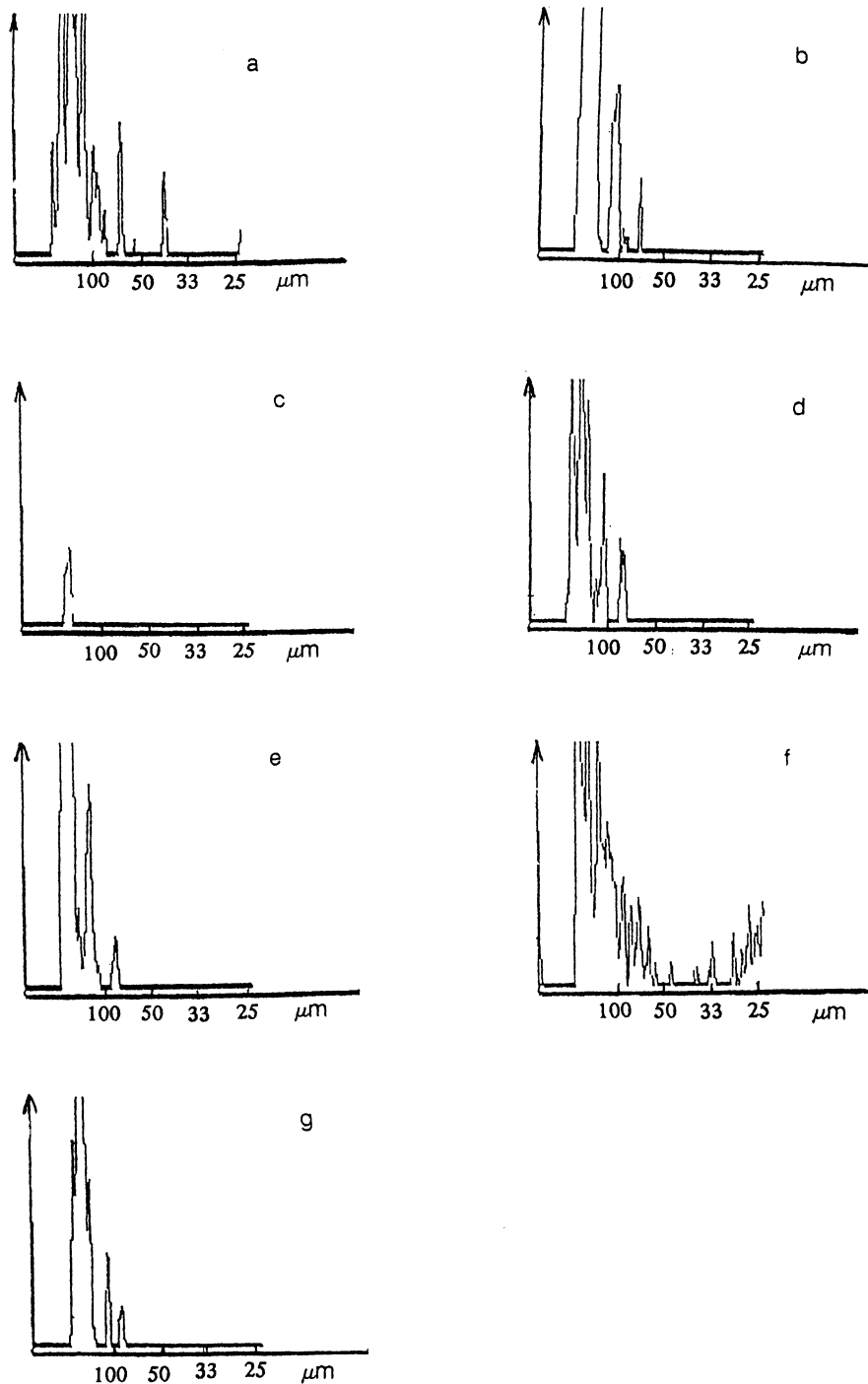


FIG. 5. Dynamics of the angular spectrum of the scattered light during spinodal decay; the times from the start of the heating are $t=1.5$ min (a); 2.8 min (b); 2.9 min (c); 3.5 min (d); 6.2 min (e); 12.8 min (f); 16.1 min (g).

2. CALCULATION OF THE PARAMETERS OF NONSTATIONARY SPINODAL DECAY IN THE EFFECTIVE FREE ENERGY APPROXIMATION

For a description of the phase state of a binary mixture one uses as a starting point in this approximation the functional (see Ref. 8):

$$F = \int dV [f(u) + K(\text{grad } u)^2], \quad (1)$$

where the order parameter u is the density of one of the components of the mixture (the density of the second component is equal to $1-u$). The variation of (1) does not, in contrast to macroscopic equilibrium phase transitions, im-

mediately give the equation of motion for the order parameter: $V^{-1}\delta F/\delta u = \mu_1 - \mu_2$ is the difference of the chemical potentials of the two components. Furthermore, the mass flow of the first component is $\mathbf{J}_1 = -L\text{grad}(\mu_1 - \mu_2)$, where L is the mobility coefficient and, finally, from the continuity equation $\partial u/\partial t = -\text{div}\mathbf{J}_1$ the diffusion equation follows:

$$u_i = L\nabla^2(\partial f/\partial u - 2K\nabla^2 u). \quad (2)$$

Linearization of Eq. (2), $f = -(a/2)u^2$, $a \sim (T - T_c)/T_c$ makes it possible to determine only the boundaries of the (u, T) region of the spinodal decay.^{6,1} To study the kinetics of the decay one must take into account the nonlinearity of

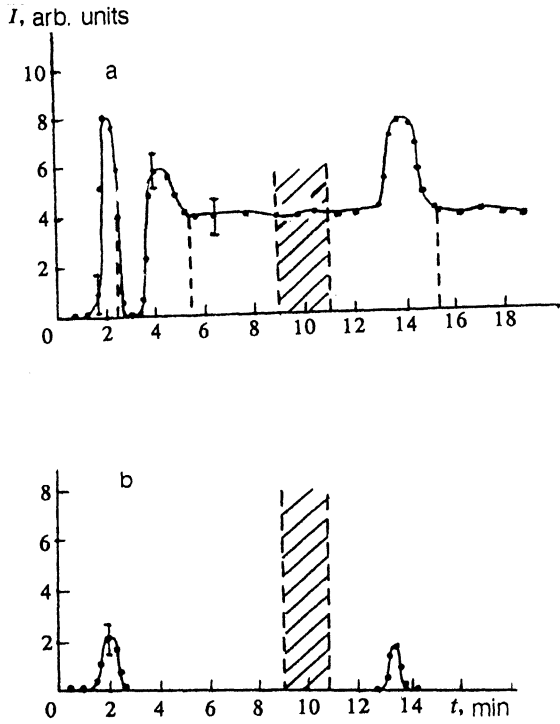


FIG. 6. Time dependence of the strength of the reflection of a structure of a fixed size: (a): $60 \mu\text{m}$; (b): $30 \mu\text{m}$; the time interval which certainly contains the moment when the thermal equilibrium is established is indicated by hatching.

f ; if one wants to take into account just the basic features of the phase transition (including a first-order one) a polynomial approximation suffices (see Ref. 8):

$$f(u) = -(a/2)u^2 + (b/3)u^3 + (d/4)u^4, \quad (3)$$

where we have $d > 0$ and the only temperature-dependent coefficient a changes sign in the critical point.

It is possible to obtain analytical stationary solutions ($\partial u / \partial t = 0$) of (2) and (3) in a one-dimensional model ($\text{grad } u = \partial u / \partial x$, where x is the spatial coordinate). They completely determine the shape of the potential

$$\left(\frac{\partial u}{\partial x}\right)^2 = (1/K)f(u) + Au + B \equiv M(u), \quad (4)$$

and, hence, the parameters of the functional (1) and the nonvanishing integration constants A and B in (2) which depend on the boundary conditions. An integral of the form (4) is also conserved for self-similar solutions (moving with a constant velocity) of (2) and (3); it therefore is meaningful to classify the solutions to be studied in wave terms.

Integration of Eq. (4) reveals three kinds of stationary solutions u_∞ . There are, firstly, solitary solutions

$$u_\infty = (1/2)(u_3 + u_2) + (1/2)(u_3 - u_2)\text{th}(\lambda_f x),$$

describing the front of the phase transition. Here the u_i are the roots of the equation $M(u) = 0$, numbered in increasing order, and we have $\lambda_f = (d/4K)^{1/2}(u_3 - u_2)/2$. Moreover, depending on the coefficients of the functional (1) and the

boundary conditions a solitary solution may be realized which has the form of a nucleus of one of the equilibrium phases:

$$u_\infty = [u_{3,2} - u_{4,1}m_b \text{th}^2(\lambda_b x)] / [1 - m_b \text{th}^2(\lambda_b x)], \quad (5)$$

where we have $m_b = (u_3 - u_2)/(u_{4,3} - u_{2,1})$ and $\lambda_b^2 = (d/8K)(u_3 - u_2)(u_{4,3} - u_{2,1})$. Here the comma between the indices means that either the first or the second indices are possible simultaneously. The third, general type of stationary solutions is periodic:

$$u_\infty = [u_2 - u_1 m \text{sn}^2(k, \lambda x)] / [1 - m \text{sn}^2(k, \lambda x)]. \quad (6)$$

Here we have $m = (u_3 - u_2)/(u_3 - u_1)$ and $\lambda^2 = (d/8K)(u_4 - u_2)(u_3 - u_1)$, while $\text{sn}(k, \lambda x)$ is an elliptic Jacobi sine of modulus $k^2 = (u_3 - u_2)(u_4 - u_1) / [(u_4 - u_2)(u_3 - u_1)]$. The spatial density oscillations (6) occur between the values $u = u_2$ and $u = u_3$; their period X is equal to:

$$X = \frac{2}{\lambda} \int_0^1 du [(1 - u^2)(1 - k^2 u^2)]^{-1/2}. \quad (7)$$

For an analysis of the nonlinear diffusion problem (2) we use the "slow period" method: we assume that the nonstationary solution has a periodic spatial dependence (6) with a period $X(t)$ which varies with time. In the calculation it is natural to transform to a time dependence $Z(t) = 1 - k^2(t)$; the vanishing of just this variable corresponds to a transition to an infinite period:

$$u = u_\infty [x, Z(\varepsilon_1 x, \varepsilon_2 t)]. \quad (8)$$

Here ε_1 and ε_2 are symbolic smallness parameters recording the conditions for the applicability of the "slow period" approximation:

$$\begin{aligned} |\partial \ln Z / \partial x| &\ll X^{-1}, \\ |\partial \ln Z / \partial t| &\ll (L/X^2) |\partial f / \partial (u^2)|, \quad LK/X^4. \end{aligned} \quad (9)$$

We carry out the evaluation of $Z(t)$, substituting (8) into (2) and using (9) to average over the spatial period X . We deduce the explicit analytical expressions for $Z(t)$ in the region near the spinodal (which is of special interest for us) where $|Z| \ll 1$ and therefore Z satisfies there the weakly nonlinear asymptotic equation:

$$\frac{\partial Z}{\partial t} = p_1 \left(\frac{\partial Z}{\partial x}\right)^2 + \frac{p_2}{2} \frac{\partial^2 Z}{\partial x^2} - \frac{p_3}{3} \frac{\partial Z}{\partial x} \frac{\partial^3 Z}{\partial x^3} + p_4 \frac{\partial^4 Z}{\partial x^4}. \quad (10)$$

The effective values of the coefficients in (10) are

$$\begin{aligned} p_1/L &= (-a + 2bu_1 + 3du_1^2) \left[\frac{1}{4} + 4D + m/(1-m)\right] \\ &\quad + (u_2 - u_1)(b + 3du_1) \left[\frac{1}{2} + 8D\right] / (1-m) \\ &\quad + 3m/(1-m)^2 + d(u_2 - u_1)^2 [12(1/16 \\ &\quad + D)/(1-m)^2 + 6m/(1-m)^3], \end{aligned}$$

$$\begin{aligned} p_2/L &= (-a + 2bu_1 + 3du_1^2) + [2(u_2 - u_1)(b + 3du_1) / \\ &\quad (1-m)] + [3d(u_2 - u_1)^2 / (1-m)^2], \end{aligned}$$

$$p_3/L = 72K\{\frac{1}{16} + D + [m/4(1-m)]\},$$

$$p_4/L = -2K,$$

where we can estimate $D = \lim_{x \rightarrow \infty, Z \rightarrow 0} \partial^2 \text{sn}(x, Z) / \partial Z^2$ by calculating the values of the coefficients in the polynomial $M(u) = (d/4K)(u-u_0)^4 - (a/2K)(u-u_0)^2 + A(u-u_0) + B$, averaged over the spatial period, near the initial density u_0 . This estimate gives $A \approx 0$, $B \approx a^2/8dK$, so that $u_1 - u_0 \approx -1.3(a/d)^{1/2}$, $m \approx 0.55$, and $u_2 - u_1 \approx 0.75(1/d)^{1/2}$.

The solution of Eq. (10), in accordance with the approximation (9), is a sum $Z = Z_0 + \xi$ where the background quantity Z_0 is described by the equation $\partial Z_0 / \partial t \approx p_2 \partial^2 Z_0 / \partial x^2$. For the perturbation of the Gaussian profile we get

$$Z_0(t, x) = \mu(2\pi)^{-1/2} (\Delta + p_2 t)^{-1/2} \times \exp[-x^2 / (\Delta + p_2 t)],$$

where μ and $\Delta^{1/2}$ are the amplitude and width of the perturbation of the stationary periodicity. Successively using the approximation (9) we linearize (10) in ξ ; this leads to an Airy equation with the solution:

$$\xi = c(p_3 q t)^{-1/3} \text{Ai}[(x + p_1 q t)(p_3 q t)^{-1/3}]. \quad (11)$$

The unimportant constant c is here determined by the initial condition; as the decisive factor we have here the coefficient q which depends on the parameters of the background perturbation. It has the meaning of an average spatial derivative $\partial Z_0 / \partial x$; in the approximation (9) used here we have $q = 0.13(\mu/\Delta)$.

It is just (11) which gives us the required result: the spatial period of the density distribution changes quasiperiodically with time, asymptotically tending to a stationary value. Here the time dependence of the quasiperiod \mathcal{T} is slow:

$$\mathcal{T}_n = 7.7 y_n (p_3 / p_1^4)^{1/3} (\Delta^{7/6} / \mu), \quad (12)$$

where $y_1 = 2.30$, $y_2 = 2.70$, $y_3 = 4.05, \dots$ are the zeroes of the Airy function. The dependence of the quasiperiod both on the material constants which depend on the model of the phase transition ($p_{1,3} = p_{1,3}(a, b, d, K, L)$) and on the boundary and initial conditions (through Δ and μ) has here been calculated approximately; one can now explicitly indicate the smallness parameter for (9): $X \ll (p_3 q T)^{1/3} = (p_3 p_1^{-4} \Delta^{7/2})^{1/9}$. Since we have $\Delta \sim l$, where l is the maximum size of the cell (≥ 1 cm) this condition is, according to our estimates, certainly satisfied near the spinodal. It is

important to note that a measurement of the period of the observed nonlinear density oscillations (of course, simultaneously with a numerical refinement of the theory and of the performance of the experiment under varying conditions) makes it possible to obtain yet another (together with X) combination of the unknown constants of the phase-transition model.

CONCLUSION

One thus observes a stratified mixture in the labile region together with "upward" diffusion and a quasiperiodic temporal "restorability." This property of nonlinear systems is atypical for diffusion processes which simulate equilibrium phase transitions, so that a detailed study of a wide class of similar physical problems seems promising for refining the general mechanism of nonequilibrium behavior. Here, clearly, one needs a more general analysis than the one given above of the model (1), which takes into account the multi-dimensional geometry. There exist well developed methods (see Ref. 9) for treating the effect of the boundary conditions for equations such as (2). Under the conditions of our experiment (Sec. 1) taking this into account must be reduced to an analysis of thermal balance, i.e., of an explicit (and nonstationary) temperature dependence of the parameters of the model (in the first place, the critical parameter a). In this connection it is useful to carry out similar experiments under nonuniform heating conditions, and the consequences of this may be the appearance of Benard-like structures (see, e.g., Ref. 7).

We note, finally, that the observed "restorability" property in spinodal decay must also be displayed by other systems undergoing a phase transition; a necessary condition for this is, apparently, that the phase separation mechanism be nonlocal.

¹ V. P. and A. V. Skripov, Usp. Fiz. Nauk **128**, 193 (1979) [Sov. Phys. Usp. **22**, 389 (1979)].

² B. Chu, E. J. Schoens, and M. E. Fisher, Phys. Rev. **185**, 190 (1969).

³ A. V. Antonov, N. F. Bunkin, A. V. Lobeov, and G. A. Lyakov, Zh. Eksp. Teor. Fiz. **99**, 1718 (1991) [Sov. Phys. JETP **72**, 959 (1991)].

⁴ O. M. Atabaev, A. A. Saidov, P. A. Tadzhibaev, Sh. O. Tursunov, and P. K. Khabibullaev, Dokl. Akad. Nauk SSSR **315**, 889 (1990).

⁵ J. S. Huang, I. Goldburg, and A. W. Bjerkaas, Phys. Rev. Lett. **32**, 921 (1974).

⁶ J. W. Cahn, Acta Metall. **9**, 795 (1961).

⁷ A. V. Gaponov-Grekhov and M. I. Rabinovich, Usp. Fiz. Nauk **128**, 579 (1979) [Sov. Phys. Usp. **22**, 590 (1979)].

⁸ L. D. Landau and E. M. Lifshitz, *Statistical Physics*, Nauka, Moscow (1976) [English translation published by Pergamon Press, Oxford].

⁹ G. A. Lyakhov and Yu. P. Svirko, Kvantovaya Elektron. (Moscow) **8**, 2245 (1981) [Sov. J. Quantum Electron. **11**, 1371 (1981)].

Translated by D. ter Haar